MARY KAY O'CONNOR PROCESS SAFETY CENTER
TEXAS A&M ENGINEERING EXPERIMENT STATION

20th Annual International Symposium
October 24-26, 2017 • College Station, Texas

CFD Modeling of LNG Flammable Vapor Cloud Dispersion

Maged Ismail[1], Srikanth Swamy[2], Alex Graham[3], Sridhar Hari[2] and Matt Straw[4]

1- *Siemens PLM Software, Houston, USA*
2- *Siemens PLM Software, Bangalore, India*
3- *Siemens PLM Software, London, UK*
4- *Norton Straw Consultants, Derby, UK*

Presenter e-mail: maged.ismail@siemens.com

Abstract

The simulation of LNG flammable vapor cloud dispersion plays a key role in the safe design of LNG terminals and other facilities. With large scale and often complex release scenarios, the scope for model testing is limited and so computational fluid dynamics (CFD) offers a valuable predictive tool, particularly where uneven terrain or obstructions are present and simpler simulation methods may be insufficient.

In this study, CFD is used to simulate a range of published LNG vapor and other dense gas dispersion experiments. Details of the setup used to model both the model scale and full scale releases included in the different datasets is presented with emphasis placed on the key model setup choices made in each case. In particular, factors such as the computational mesh and processing and interpretation of data from the completed run were examined.

Finally, the numerical results computed are compared with experimental point-wise and arc-wise maximum concentration data to validate the CFD models. The individual challenges presented by each dataset and ability of the CFD model to reproduce experimental measurements in each case is analyzed and discussed.

Introduction

In any computational modelling effort, modelers make reasonable assumptions that assist in simplifying the problem to a level where numerical solutions can be attempted to closely predict the reality. A process known as Verification and Validation (V&V) [1], has been developed by the

modelling fraternity to examine how reasonable and accurate computational models are in their predictions, both from a qualitative and quantitative perspective.

Generally, Verification is the process of checking that the computational implementation of a model accurately represents its mathematical basis, i.e. that the model equations have been coded correctly. One approach is to compare predictions from the computational model for select problems for which there exist known analytic solutions. Typically, tool developers have standard sets of such exercises that are used to repeat test each released version of the tool.

Validation is the next step and a more rigorous examination wherein predictions are sought from computational models for sets of typical field experiments with different variations. Canonical data exists in literature discipline-wise which different tool developers choose to validate their predictions and demonstrate how theirs' compare against experimental data as well as their competition. As typical commercial tools encompass a variety of models that cater to different technical disciplines, not each of them get validated at the source of their implementation. It is seen that tool users resort to performing validation exercises for models that are relevant and important for their area of work, before embarking on its use internally.

Validation of atmospheric dispersion models is not straightforward. Compared to many fields of engineering, acceptance standards for validation of atmospheric dispersion models are relaxed. Commonly, a model may be considered to provide acceptable performance if predictions are within a factor of two of the measurement data. This in part reflects the level of uncertainty in many of the sets of measurement data.

In response to an increase in the design and construction of LNG terminals, a study was commissioned by Pipeline and Hazardous Materials Safety Administration (PHMSA) to establish the viability of numerical modelling tools for modelling accidental releases. This resulted in the 'Model Evaluation Protocol (MEP)' [2] encompassing a comprehensive survey of existing models and datasets for validation (33 test cases of different types). Any model can be validated by following the processes outlined in this document; the shortcoming however being that there is a limited number of accepted models. In a more recent work [3], the authors have carried forward their previous effort by devising a comprehensive evaluation protocol that meets new industry standards developed especially for the assessment of LNG vapor dispersion models, including a supporting suite of validation data and guidance on the use of this data.

A review of the recent literature [4, 5] indicates that increasing efforts are being devoted to using computational modelling techniques for this application. This is not very surprising as the last decade has seen a significant increase in availability of computing resources (both hardware and software). From a time where most of these analyses were primarily one-dimensional in nature a couple of decades ago, we have sophisticated three-dimensional computational fluid dynamics (CFD) tools such as ANSYS-FLUENT [6] and STAR-CCM+ [7] available to be utilized for the modelling effort now. Besides being current state-of-the-art and highly user-friendly, these tools are capable of being run in parallel, high-performance computing (HPC) platforms that facilitates these types of complicated analyses.

Details of the Model Evaluation Protocol were recently reviewed by Siemens Industry Software Limited (formerly CD-adapco) with an intention to initiate efforts to assess suitability of our flagship computational fluid dynamics (CFD) tool STAR-CCM+ for this modelling effort. As a first step in this direction, we have chosen a couple of validation exercises (one each from two different type of validation cases): field trials and wind tunnel trials from a suite of exercises available in the MEP literature.

We commence this effort by having a short discussion on the comparable value obtainable from wind tunnel tests vs field trials and also introduce the challenges related to each of the above. In the next section, we provide a brief introduction on each of the cases that includes background information, description, set-up and methodology employed in performing the simulation and conclude by presenting results of our investigation followed by a discussion. As the study is primarily computational in nature, we have also attempted to address a couple of important factors relevant to the investigation, as mentioned below:

- Sensitivity of the results to the computational mesh in the CHRC case
- Handling wind variance in Burro Sands

LNG Hazards – What needs to be modelled?

LNG spills typically result in a boiling pool of cold liquid which evaporates at a certain rate. The underlying physical process in this scenario is fairly complex and involves multiphase flow with rapid phase change and heat transfer. This problem is hence a challenging and expensive modelling proposition and not a simulation that would be undertaken on an everyday basis.

It is common practice within the modelling community to simplify the original problem that encompasses complex physics of the spill by excluding the phase-change part of the problem and starting the modelling effort by assuming a gas source. Further, the simplified problem can be decomposed into two parts: Source modelling (first part) and Dispersion modelling (second part). In other words, spilled fluid is modelled as a gas species source in the simplified CFD problem: simulation starts from production of the gas (from pool evaporation) and proceeds to address dispersion of produced gas in the ambient environment due to underlying convection and diffusion processes. One additional piece of information, a sub-model providing information on the production rate of gas is required to close the loop.

Modelling LNG dispersion under the CFD framework can be thought of to be both a simple and a complex problem based on the perspective chosen to review it. It is simple for the reason that underlying physics can be treated as single-phase transport under the multi-component (multi-species) framework, and, simulation domain would usually not be complicated (unless there is a need to address complex structures such LNG terminal infrastructure or offshore platforms). However, features such as the presence of an atmospheric boundary layer (ABL) and the associated density stratification and turbulence, combination of large and small scales due to geometrical enormity, and existence of wide temperature gradients (Spill fluid temperature ~111 K and Ambient Temperature ~300 K) within the computational domain introduce their share of modelling complexity.

Wind Tunnel Tests vs Field Trials

Experimental data presented in the MEP [2] fall into two categories namely (a) Field Trials, and (b) Wind-Tunnel trials. However, a quick summary characterizing each is presented below:

Field Trials

(a) Mostly unobstructed releases over land and water
(b) Spill itself always onto a pond of water
(c) Falcon trials do include obstructions in the form of a containment fence and billboard

Wind Tunnel Trials

(a) Model scale tests and hence are characterized by lower Reynolds number values
(b) Combination of unobstructed and obstructed releases
(c) Obstructions mainly in the form of fences that are located either upstream or downstream of the release locations.
(d) CHRC tests include a containment dike and storage tank.

The choice of validation exercises were made based on a careful consideration of various factors related to availability of geometry as well as data for a range of field variations that can be modelled and predictions compared against: Specifically, geometric details of the CHRC case are well-defined and are easily re-cast for the CFD study. Out of the field trials, wind variance in the Maplin sands case is low while that for the burro case is high. Further, short time-averaged data is available for the former while both short and long time-averaged data is available for the latter. As can be seen from the description, a combination of the above set of parameters is an excellent test of the software capability.

Description of cases chosen for validation in the current effort and documented in the MEP [2]; elaborate details are available in the individual publications that are provided in the reference section of the MEP and are not reproduced independently here.

Wind Tunnel Tests

CHRC Tests

Background

These tests were performed at the wind tunnel facility in Chemical Hazards Research Center (CHRC) at the University of Arkansas, USA. In these tests, dispersion of carbon dioxide in the wind tunnel under three different conditions were studied with an aim to generate validation data for a computational model.

Description

The wind tunnel was an ultra-low-speed boundary-layer wind tunnel capable of simulating the constant stress layer of the atmospheric boundary layer. Airflow from the driving fans passed through a circular-to-rectangular transition to a 7 × 20 × 80 foot working area in which the floor was covered with smooth rubber matting on which roughness elements were mounted. The measurement region begins ~18 ft. downwind from the end of the rectangular region.

The experiments were at a scale of 150:1; following three cases were simulated:

Case A: Low-momentum area source CO_2 release without obstacles.
Case B: Low-momentum area source CO_2 release with tank and dike.
Case C: Low-momentum area source CO_2 release with dike only.
Following information was maintained constant for the cases:
Source area, Spill rate, Wind speed (and inlet profile) and Leak: CO_2 (density ~1.7x that of air)

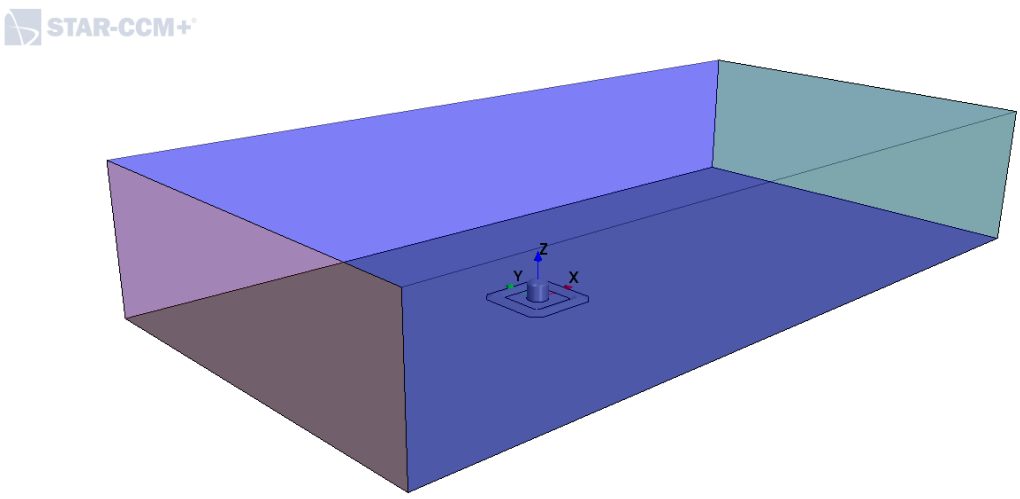

Figure 1. Computational domain for CHRC B configuration

Computational domain

The dimensions of the computational domain were made large enough to avoid effects of side and top boundaries. The computational domain extended from -4.5 m to 7.5 m in flow direction, from 0 to 2.1 m in vertical direction and from -3 m to 3 m in lateral direction, respectively. Figures 1 and 2 present salient features of computational domain with important details that attempt to closely follow the actual test details.

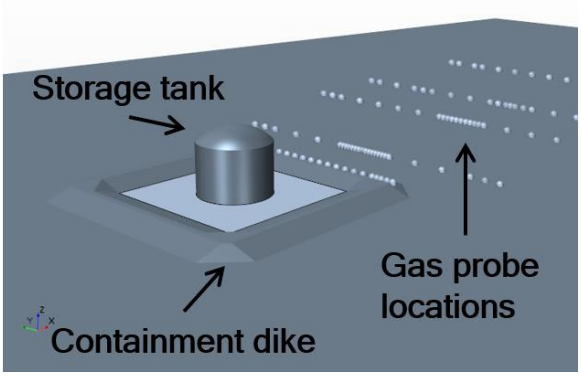

Figure 2. Close-up view of geometrical details for CHRC B configuration

Meshing

In this study we used a meshing approach utilizing the unstructured trimmed cell mesher and the prism layer mesher in STAR-CCM+. The trimmed mesher generates predominantly hexahedral cells with minimal cell skewness and automatically refines the mesh on curved surfaces. Anisotropic mesh refinement was applied in the wall-normal direction to resolve the atmospheric boundary layer (ABL) profile as well as local boundary layer flows in the vicinity of the tank and dike. For the prism layer mesher, the number of prism layers along walls was set to 8 and the total prism layer thickness was set to 5 mm. A side view of the mesh illustrating the mesh refinements near the wall and the obstruction geometry is presented in Figure 3.

Boundary conditions

The following boundary conditions were applied to the computational domain:

- Velocity inlet boundary condition at the upstream boundary;
- No-slip wall on the ground, tank and dike boundaries. A surface roughness height value of 7.2e-4 is applied to the ground wall boundary;
- Symmetric condition at both lateral side boundaries and top of the domain;
- Flow-split outlet at the downstream outlet boundary.

Physics models and solvers

The CFD analysis was run using the Steady Segregated Flow solver in STAR-CCM+ v12.04. CO_2 concentrations at probe locations were tracked with respect to iterations and the simulations were run until they reached steady values. The Reynolds Stress Turbulence model with all-y+ wall treatment was selected for modelling turbulence. The working fluid was defined as multi-component gas, composed of CO_2 and Air. The Segregated Species solver was used for modelling the species transport of the two gas species. The densities of the two species were assumed to be constant and the flow was assumed to be isothermal.

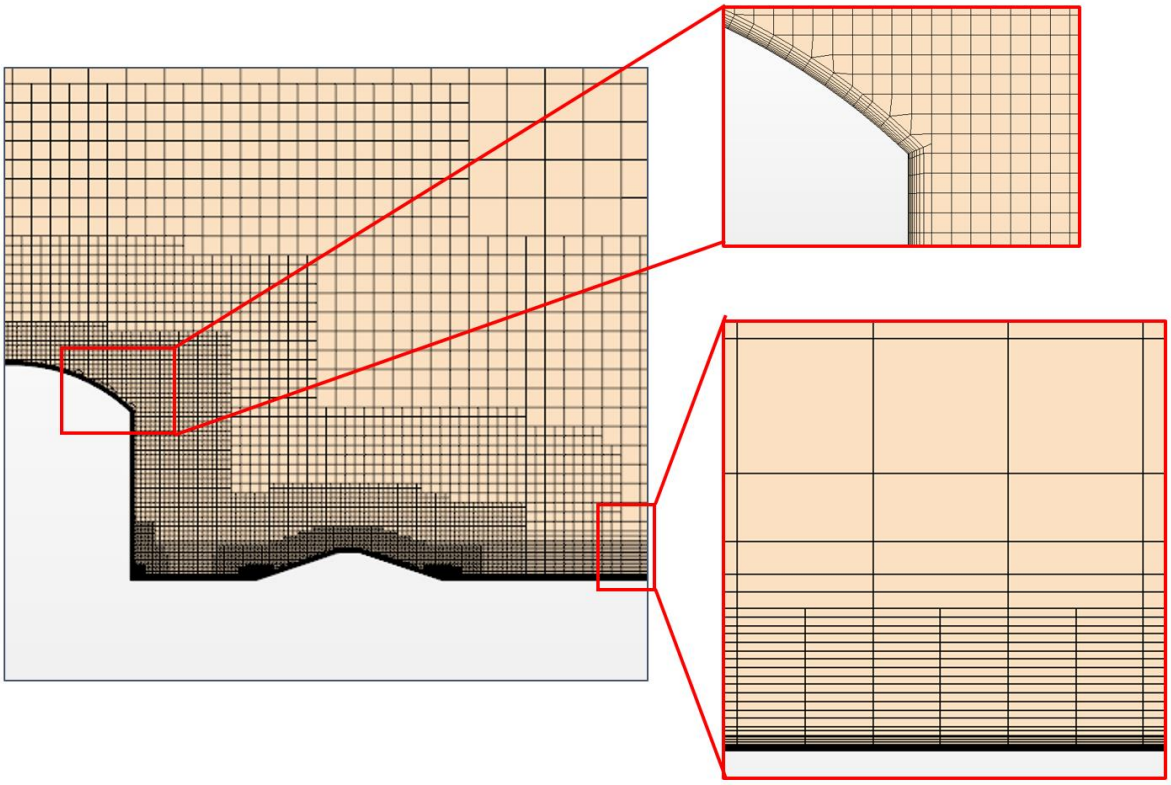

Figure 3. Side view of mesh illustrating refinement in the vicinity of the wall, tank and dike

Results

Mesh refinement convergence

The effects of mesh resolution on the predicted concentration results were analyzed by performing simulations on systematically refined grids. The CHRC configuration B was selected as a suitable test case for the mesh refinement study, since it includes important geometrical details, i.e. the tank and dike, which require more careful consideration of mesh settings. The mesh base size was reduced by a factor of 2 in the entire computational domain, except in the prism layer cells along walls, where the refinement was only in the directions tangential to wall. As a quantitative measure to compare results on different mesh resolutions we calculated the difference between the predicted and measured maximum arc-wise concentrations. The average (arithmetic mean) of the percentage difference was then calculated and reported in Table 1 below. Generally, we observed a trend that predicted concentrations were in better agreement with measured data as the mesh was refined. It was decided that the Fine mesh configuration provides good compromise between accuracy and computational cost. For the rest of simulation test cases reported in this section, the same mesh settings for the fine mesh were used.

Table 1. Effect of mesh resolution on maximum arc-wise concentrations

Mesh Configuration	Base Size (m)	Cell Count (million)	Average of % Difference to Measurements
Coarsest	0.8	1.7	12.5%
Coarse	0.4	2.3	10.8%
Intermediate	0.2	3.7	11%
Fine	0.1	9.6	8.1%

Maximum Arc-wise Concentrations

Figures 4 through 6 show comparison between measured and predicted maximum arc-wise concentration for the three CHRC trial cases. Results overall show high level of agreement with experimental data. For CHRC cases A and C, we observe that the maximum concentration values close to the CO_2 source exhibit higher discrepancy between measurements and CFD results, which suggests that more accurate approaches for source modelling might be required. In case B, a very close agreement is seen over all distances, possibly explained by the proximity of the first row of sensors to the obstructions (tank and dike).

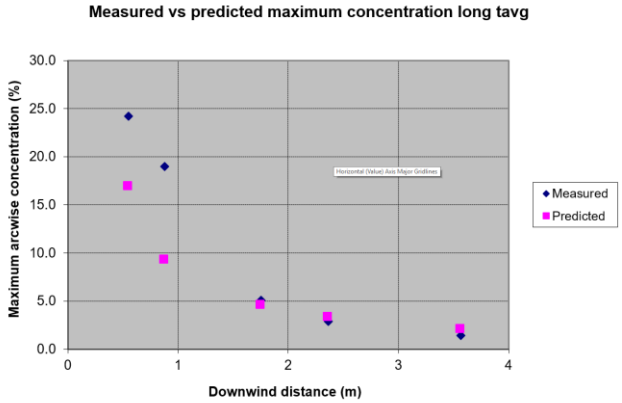

Figure 4. CHRC Case A: Unobstructed

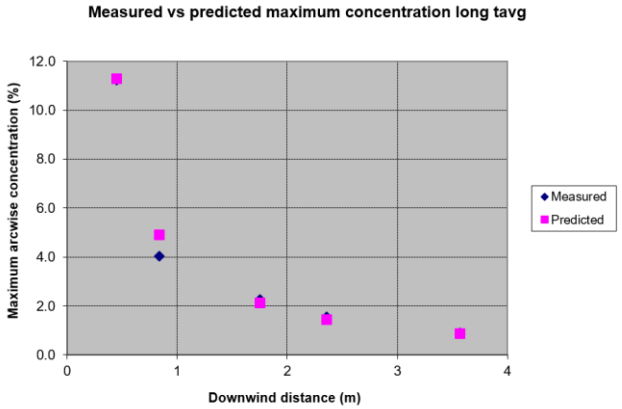

Figure 5. CHRC Case B: Tank and Dike

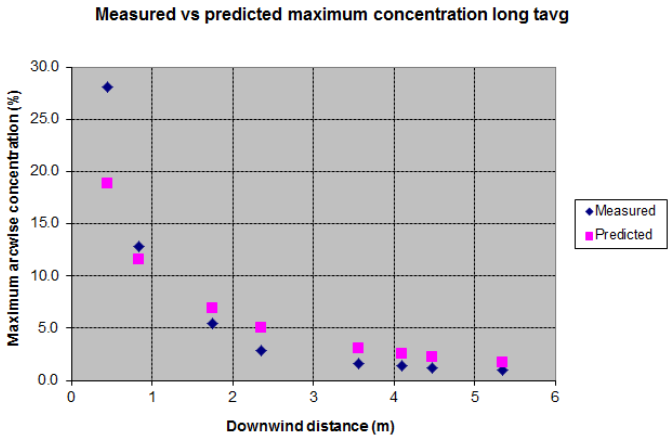

Figure 6. CHRC Case C: Dike only

Field Trials

Maplin Sands Tests

Background

The Maplin Sands trials were conducted by Shell Research Limited in 1980 and consisted of 34 spills of liquefied gases onto the sea. The aim of the trials was to study dispersion and combustion of flammable gases. Both continuous and instantaneous releases of refrigerated liquefied propane (LPG) and LNG were carried out.

Description

The arrangement of the measurement arcs around the spill point at the release site is shown schematically in Figure 7. The release point was 350 m offshore; liquid was delivered by pipeline from the onshore gas handling point. A 300 m diameter dike was constructed around the spill point to retain water whose level varied by around 0.75 m.

The release configuration involved a 150 mm diameter pipe directed vertically downward terminating above the water surface. Distance from the pipe exit to the water surface varied between tests and was recorded. Gas sensing instruments were deployed in 71 floating pontoons set in an arc around the spill point at different heights and a fast response thermocouple was also fitted close to the lowest gas sensor. Direction and magnitude of the wind speed was recorded.

Different data sets required to accurately set-up the simulation (thermodynamics and transport properties, upwind velocity/temperature profiles) as well as field data from the tests required for validation (gas concentration) have been well documented. A list of reports and manuscripts from which this data can be obtained are provided in the MEP guide for ready reference. A note on the expected uncertainty is also made.

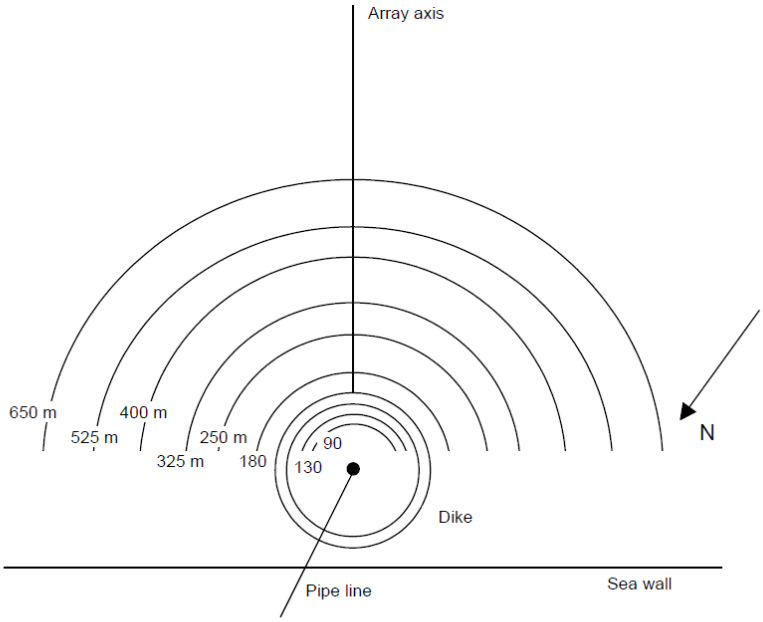

Figure 5 Maplin Sands spill area and measurement arcs

Figure 7. Maplin Sand spill area and Measurement Arcs

Computational domain

Unlike wind tunnel tests, current field trails (Maplin and Burro tests) are unobstructed releases over land and water. Figure 8 represents the simulation domain which was created in STAR-CCM+ with the following dimensions 600m×1200m×250m in the X, Y and Z axes, respectively.

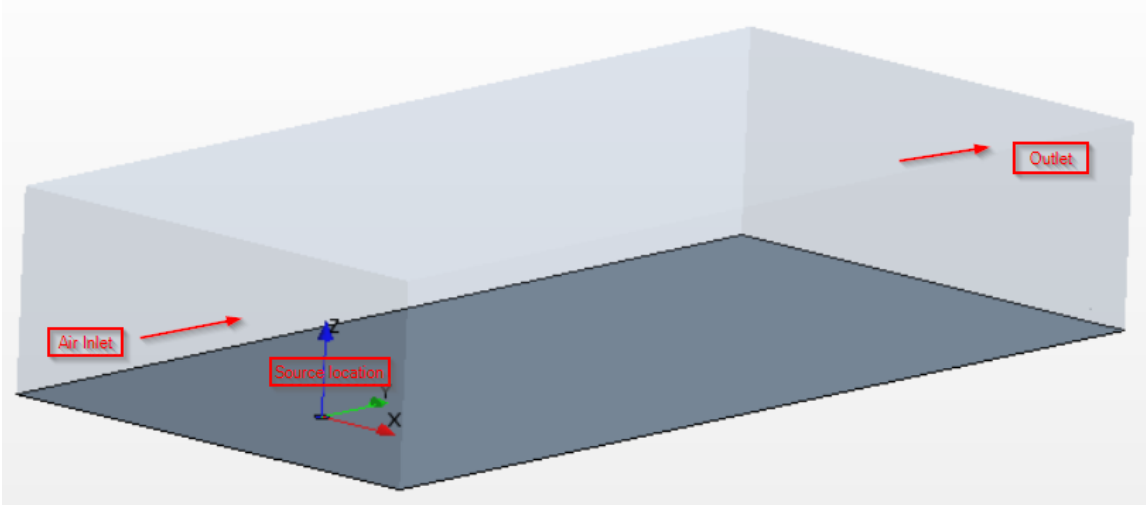

Figure 8. Computational domain for Maplin Sands configuration

Meshing

The domain is discretized with trimmed hexahedral elements as in the CHRC case. Mesh has been refined near source and dispersion area downstream to resolve expected gradients in these regions. Figures 9 and 10 demonstrate mesh refinement on the ground and a section plane passing through the source.

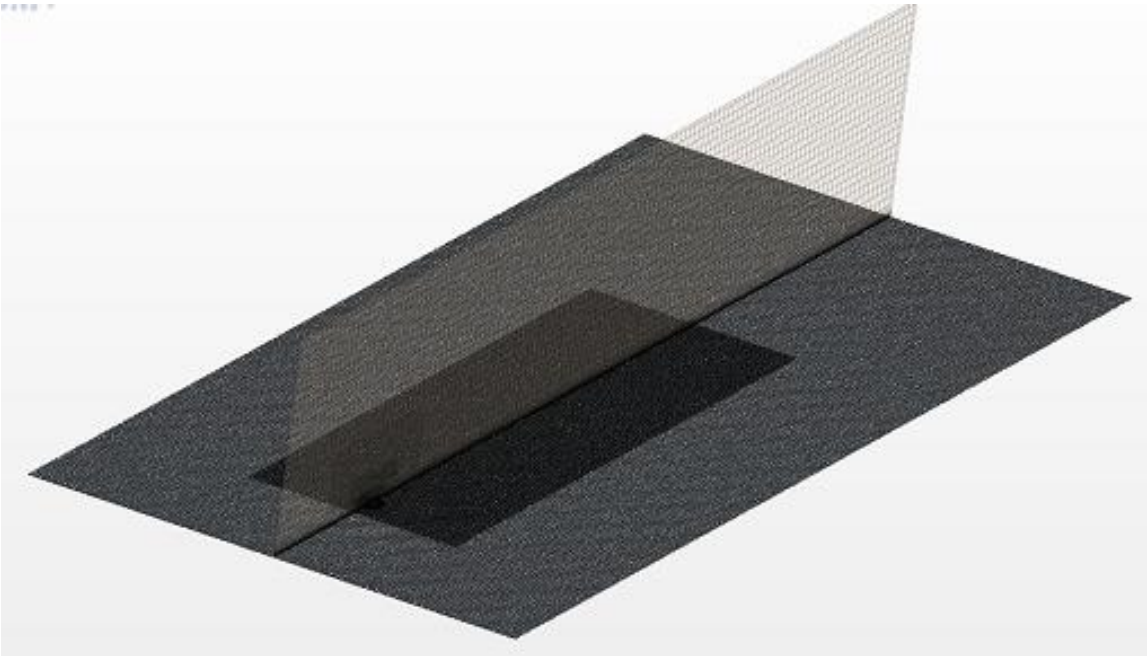

Figure 9. Side view of refinement near source.

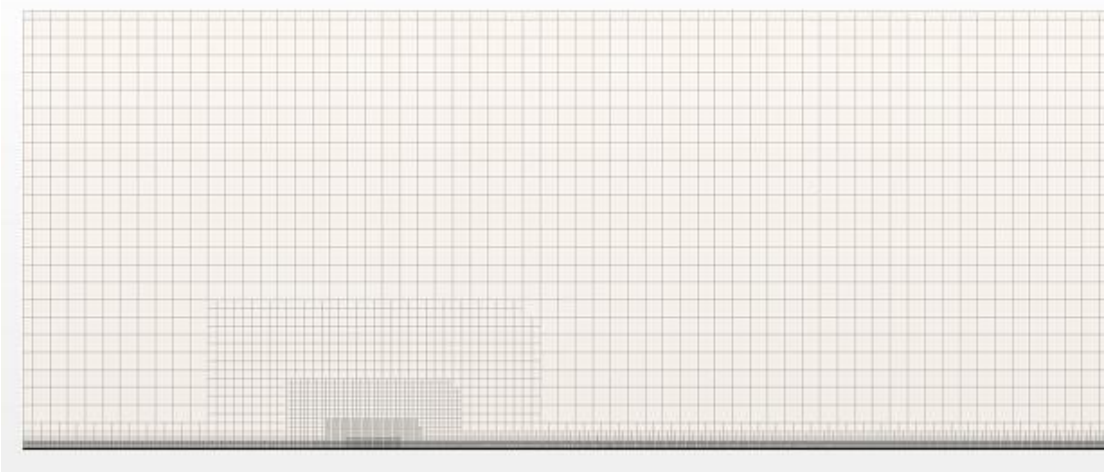

Figure 10. Refinement on the section plane passing through the source

Boundary conditions and initial conditions

The domain consists of seven boundaries. Except for the outlet and ground, every other boundary is set as a velocity boundary. The value of velocity, turbulent kinetic energy and dissipation is calculated based on the method proposed by Alinot & Masson [8] that provides velocity, temperature and turbulence profiles for the range of atmospheric stability classes. User-defined functions have been created for each profile and set under the appropriate field under inlet conditions for each boundary, as described below:

(a) A wall boundary was applied to the ground with surface roughness value 9e-3.
(b) Outlet boundary was set as pressure outlet boundary.
(c) User-defined species source term has been defined based on the source volume data provided in experiment and that is the source for the LNG release.

Solver

The case is solved as a steady-state problem and convergence is declared when values at the different probe locations reach a constant value. The Reynolds stress transport model with a Quadratic Pressure-Strain option was used to account for the fluid turbulence. A high y+ wall treatment was chosen to capture the near-wall behavior.

When the dense gas clouds disperse in the atmosphere, stable stratified layers are formed under the action of gravity, where mixing is suppressed due to the density gradients. Turbulent diffusion is responsible for a larger share of mixing and turbulent production due to buoyancy will also affect scalar fluxes. In STAR-CCM+ the Generalized-Gradient-Diffusion Hypothesis Proposed by Daly and Harlow [9] relates the eddy-diffusivity to the Reynolds Stress Tensor (Equation 1) and was enabled under quadratic pressure strain properties.

$$\overline{u_i c} = -\alpha_c \tau_c \overline{u_i u_j} \frac{\partial C}{\partial x_j}$$

Equation 1. Reynolds Stress Tensor

Standard Gradient Diffusion Hypothesis (SGDH) is based on proportionality between scalar flux and mean scalar gradient. SGDH is the method used with eddy-viscosity turbulence models and it relates scalar flux to mean concentration gradient via a constant based on the Schmidt number and the eddy-viscosity. Multi-component gas mixture has been enabled along with species segregated species model to solve the transport equations for each gas species.

Results

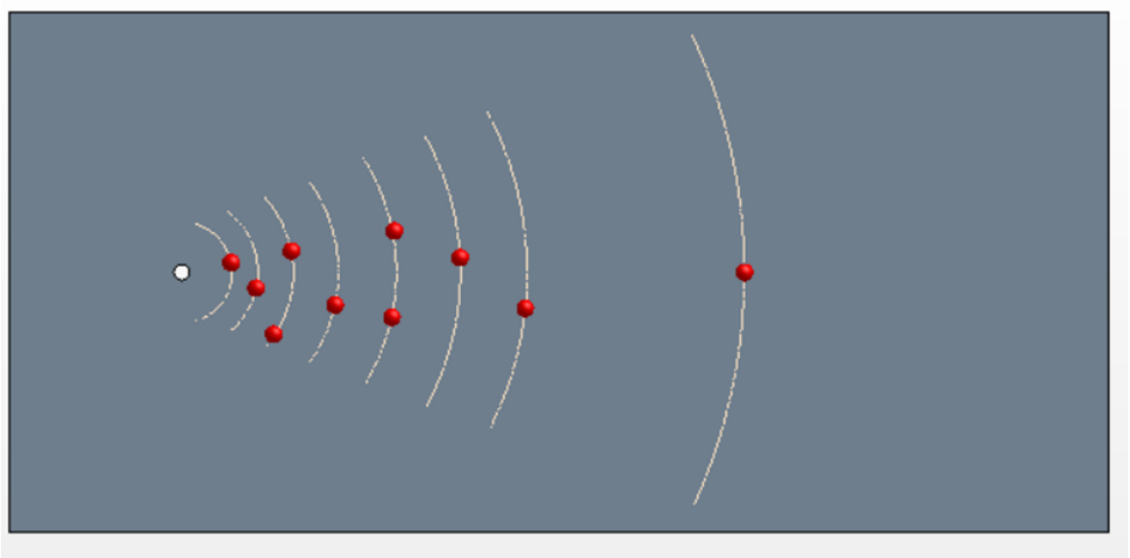

Figure 11. Location of the points on the different arc locations

Figure 11 shows a top-view of the domain to illustrate the actual point measurement locations. Experimental data is in the form of maximum arc-wise concentrations, taken from a rolling short time-average. The measurement points lie on each arc at distances measuring 58m, 88m, 129m, 181m, 248m, 322m, 399m, and 650m from the source location. Experimental results have been taken from the latest LNG model validation database.

Figure 12 through 14 provide a comparison of the maximum arc wise concentration measured with respect to the downward distance for all three tests. It can be seen from Figures 12 through 14 that there is a fairly close agreement between experiment and CFD arc-wise maxima. For this analysis, CFD runs have been performed in steady-state (instead of unsteady) to obtain the short-time average values, despite the fact that a steady state solution would generally be considered more suitable for assessing the long time-averaged situation. The justification is that, by taking the maximum over a continuous arc (i.e. the centerline concentration) rather than over a range of discrete points, the fact that the wind is meandering during the test can be disregarded in this case.

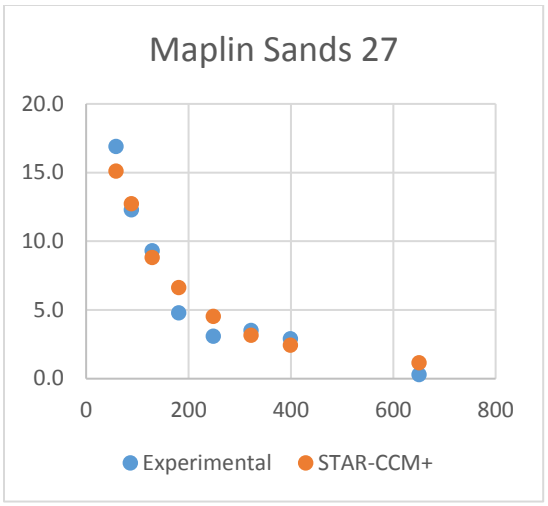

Figure 12. Comparison of Predictions to Experiments for Case 27

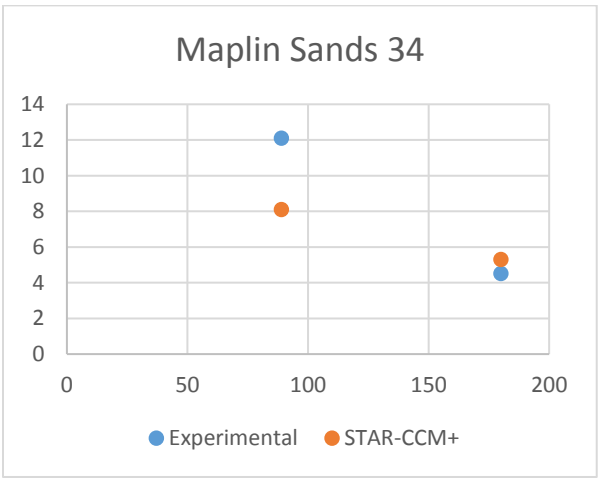

Figure 13. Comparison of Predictions to Experiments for Case 34

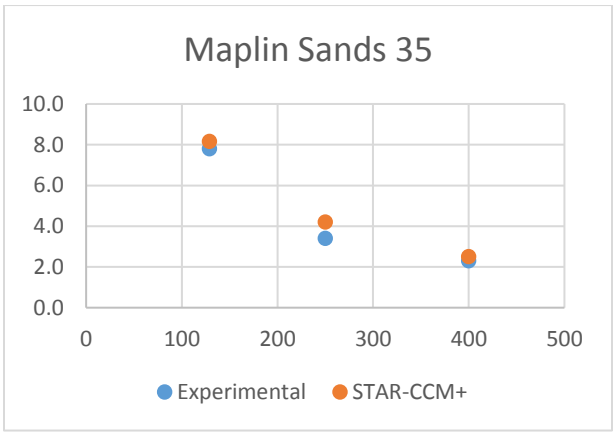

Figure 14. Comparison of Predictions to Experiments for Case 35

This approach removes the need for the wind fluctuations to be faithfully reproduced in time and space at each individual sensor location, requiring possession of time-accurate wind data and a

costly transient simulation. Measuring the arc-wise maxima in a time accurate fashion, using the same process as in experimental trials, is not necessary if only the maximum value is of interest.

Burro tests

Background

The Burro series of experiments [10, 11] were performed at the Naval Weapons Center (NWC), China Lake, California in the summer of 1980. There were eight LNG spills of between 24 m3 and 39 m3 onto water. The arrangement of the spill area and measurement arcs is shown schematically in Figure 15.

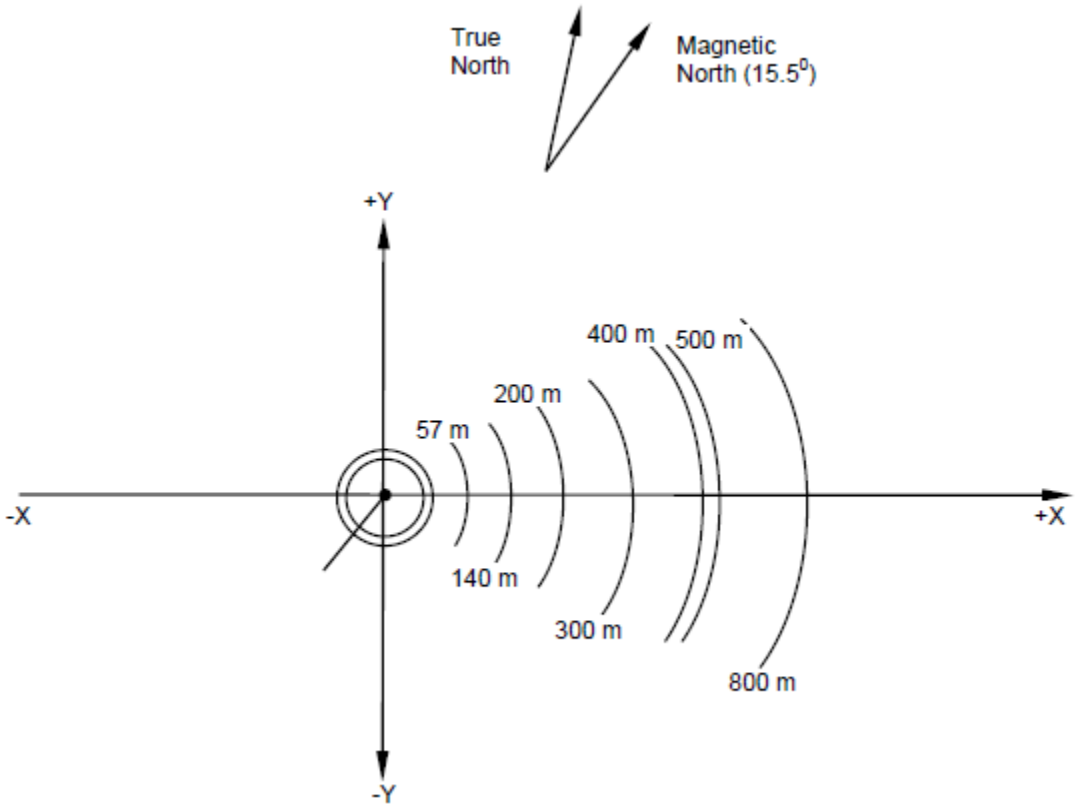

Figure 15. Burro Tests: Spill Area and Measurement Arcs

Description

The LNG was stored in a cryogenic tank capable of holding up to 40 m^3. A 25 cm diameter spill line ran from this tank to a 5.7 m^3 spill tank with valve. A further 25 cm diameter line ran from the spill valve to a water test basin, where it terminated 1.0 m above the surface of the water basin. A splash plate was fitted below this pipe outlet to limit penetration of the LNG into the water. The splash plate was located just underneath the water surface and directed the flow of LNG horizontally across the water surface. The LNG was forced out under pressure by gaseous nitrogen.

Setup/methodology

Figure 16 represents the simulation domain created in STAR-CCM+ with the following dimensions: 1100m×400m×250 m in X, Y, Z respectively. Domain, Boundary and Initial conditions were maintained the same for all the Burro test series (3, 7, 8, and 9) with only differences in source volume, properties, atmospheric conditions and probe locations.

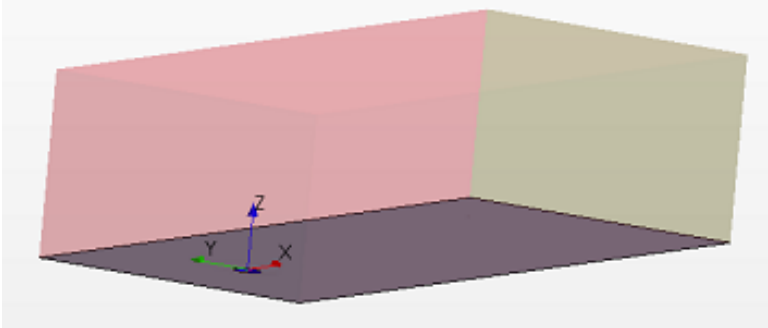

Figure 16. Computational domain for Burro Tests configuration

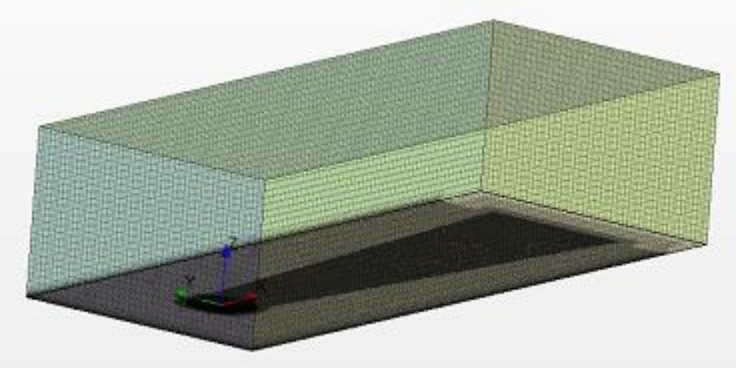

Figure 17. Volumetric Mesh with Source Refinement

Results

Figure 18 show a top-view of the domain to illustrate the actual probe-point measurement locations. Since experimental results contains both short-time and long-time averaged results, prediction from simulation results has been obtained on these probe points as well maximum value from the arc-wise data.

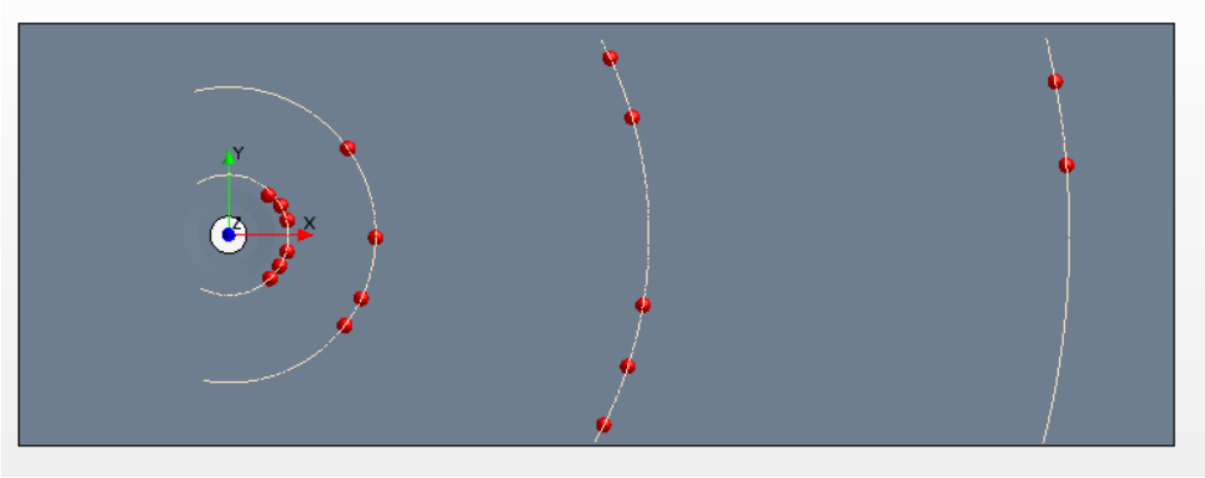

Figure 18. Location of the points on the different arc locations

Comparison to short-time averaged data:

As discussed in Maplin Sands tests, short-time averaged data has been compared with maximum value on the arc obtained from steady state simulation results for all the Burro tests as shown in Figures 19 and 20.

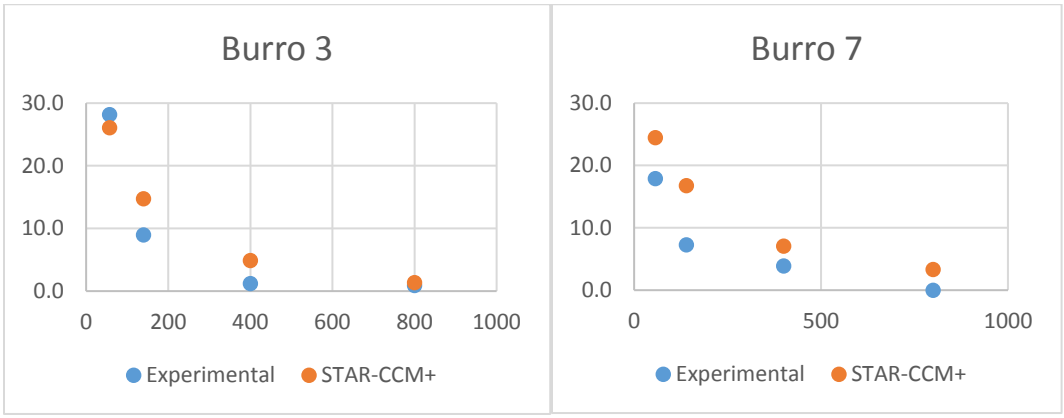

Figure 19. Comparison of Predictions to Burro Test data: (a) Test 3 (L), and (b) Test 7 (R)

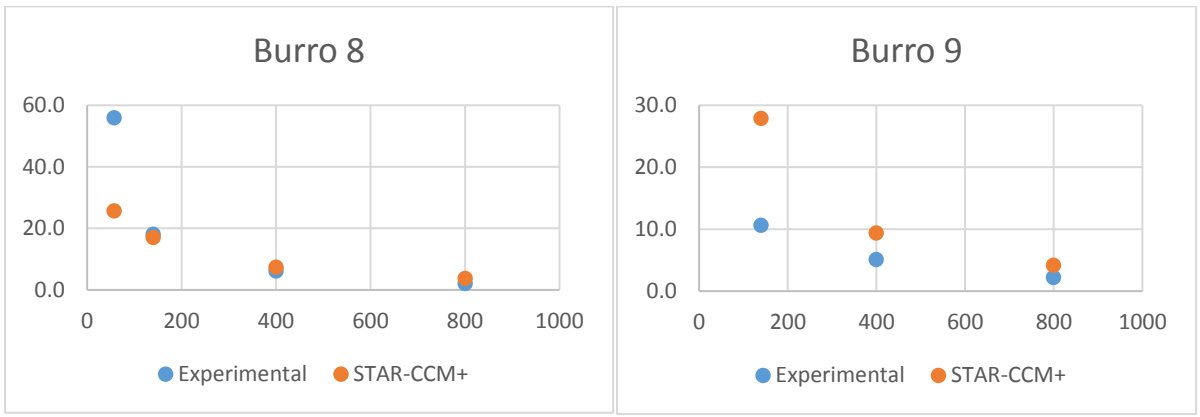

Figure 20. Comparison of Predictions to Burro Test data: (a) Test 8 (L), and (b) Test 9 (R)

Comparison to long-time averaged data:

For Burro tests, experimental data [12] is provided with values of mean and standard deviation of wind angle due to meandering for all the cases. Due to the wind variance, long-time averaged concentration measurements will be lower as the turbulent fluctuations giving rise to short term peaks are averaged out since the plume passes close to a given point for only a portion of the time measured.

To account for this variance, assuming a Gaussian distribution of wind angles along with standard deviation, the cumulative density function (CDF) is calculated and used to determine a probability that the wind direction will lie within a certain range of angles.

The products of the predicted concentrations from steady state runs at a series of different wind angles with the weights obtained from the CDF can be summed together to produce a long term average. In our study, runs were conducted over a range of 4σ on both sides of the mean wind angle for Gaussian distribution. Results of above exercise presented in Figures 21 and 22 show a fair comparison to experiment values for the long time-averaged data and agreement improves with distance from the source

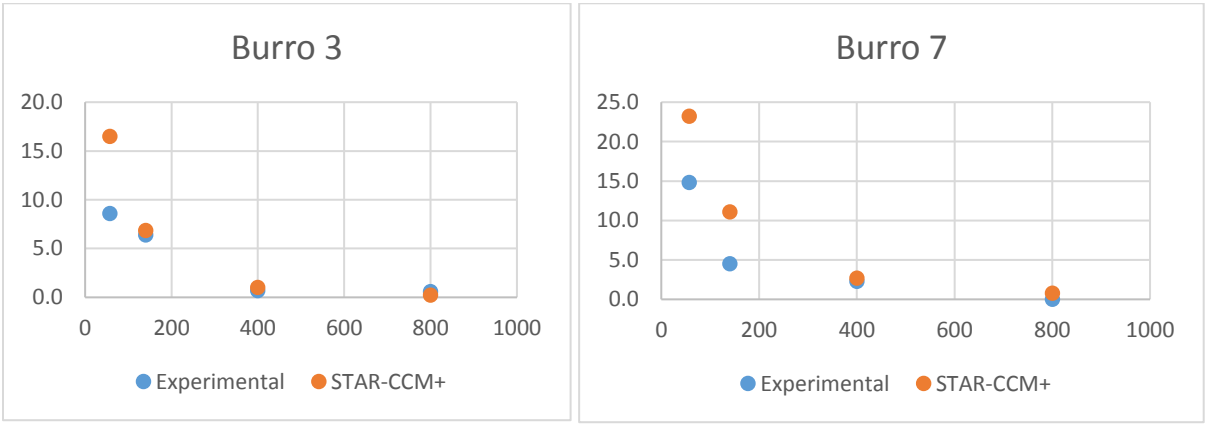

Figure 21. Comparison of Predictions to Burro Test data: (a) Test 3 (L), and (b) Test 7 (R)

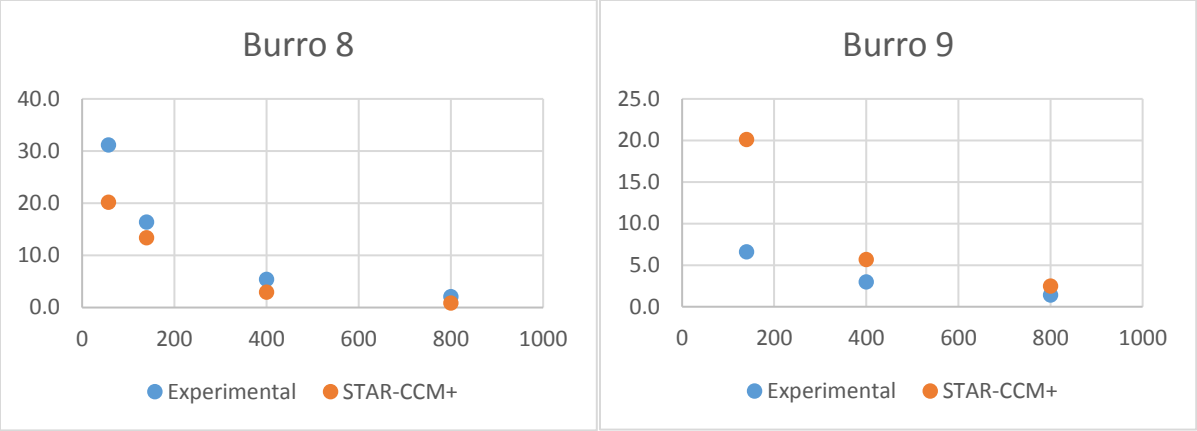

Figure 22. Comparison of Predictions to Burro Test data: (a) Test 8 (L), and (b) Test 9 (R)

Conclusions

In this effort, we have attempted to investigate suitability of Siemens Industry Software CFD tool STAR-CCM+V12.04 to model problems involving atmospheric dispersion of LNG following a spill event. To this end, we have identified validation exercises from precedent literature comprising both field trials and wind-tunnel tests that encompass a wide variety of process conditions.

In addition, we have also discussed certain modelling subtleties related to domain consideration, mesh generation and data interpretation to demonstrate how (a) each one of the above processes can influence the CFD predictions, and (b) be fine-tuned to attain a suitable match to the experimental results.

Following is a brief summary of our effort:

- Simulation of Wind tunnel experiment (CHRC case): CFD predictions show a favorable comparison to experimental data under conditions of controlled steady state flow.
- Field trials (Maplin Sands and Burro Tests): Though more complicated cases, predictions indicate a fairly good accuracy. Primarily, we found that
    - Use of continuous arc measurements can approximate well to short-time averaged maxima, and save a costly transient simulation using CFD.
    - Converting to long-time averaged values with the Gaussian approximation works well, assuming the sensors are all located within +/- 4σ of the mean direction (i.e., assuming the plume would actually pass over them at some stage)

In a number of comparisons slight discrepancies are noticeable close to the gas source which are likely to be more influenced by exactly how the gas is released into the domain. In some cases this is an area of uncertainty when interpreting physical test set-up and requires assumptions to be made in the modelling. Greater detail of exactly how releases were made in tests would enable further investigation into the source term modelling approach. Measurements further downstream from the source generally match well, and these more distant predictions are of more importance for predicting flammable vapor cloud size in practice.

Using just steady state runs, a good set of results are achieved for both short and long time averaged data. This is a pragmatic approach which is relevant to typical industrial cases, where generally many release scenarios and wind conditions must be covered in a single safety study.

References:

(1) *https://en.wikipedia.org/wiki/Software_verification_and_validation*

(2) M.J. Ivings, S.F. Jagger, C.J. Lea, D.M. Webber., *Evaluating vapour dispersion models for safety analysis of LNG facilities, The Fire Protection Research Foundation*, 9 May 2007.

(3) M.J. Ivings, C.J. Leas, D.M. Webber, S.F. Jagger and S. Coldrick., *A protocol for the evaluation of LNG vapour dispersion models.* Journal of Loss Prevention in the Process Industries, 2013. **26(1)**: p.153-163.

(4) W.C. Ikealumba and H. Wu., *Modeling of Liquefied Natural Gas Release and Dispersion: Incorporating a Direct Computational Fluid Dynamics Simulation Method for LNG Spill and Pool Formation*. Industrial and Engineering Chemistry Research, 2016. **55**: p.1778-1787.

(5) F. Nazarpour, J. Wen, S. Dembelea and I.D. Udechukwua., *LNG Vapour Cloud Dispersion Modelling and Simulations with OpenFOAM*. Chemical Engineering Transactions, 2016. **48**: p.967-972.

(6) *ANSYS FLUENT, Canonsburg, PA. http://www.ansys.com/.*

(7) *STAR-CCM+ Version 12.04, Siemens Industry Software Ltd.*

(8) S. Alinot and C. Masson., *k-ε Model for the Atmospheric Boundary Layer Under Various Thermal Stratifications*. Journal of Solar Energy Engineering, 2005. Trans ASME, **127**: p.438-443.

(9) B.J. Daly and F.H. Harlow., *Transport Equations in Turbulence*, Physics of Fluids, 1970. **13**: p.2634-2649.

(10) R.P. Koopman, R.T. Cederwall, D.L. Ermak, H.C. Goldwire Jr, W.J. Hogan, J.W McClure, T.G. McCrae, D.L. Morgan, H.C. Rodean and J.H. Shinn., *Analysis of Burro series 40 m3LNG spill experiments*. Journal of Hazardous Materials, 1982a **6**: p.43-83.

(11) R.P. Koopman, J. Baker, R.T. Cederwall, H.C. Goldwire Jr, W.J. Hogan, L.M. Kamppinen, R.D. Kiefer, J.W McClure, T.G. McCrae, D.L. Morgan, L.K. Morris, M.W. Spann Jr and C.D. Lind., *Burro series data report LLNL/NWC 1980 LNG spill tests*, UCID-19075, Vols 1 & 2, Lawrence Livermore National Laboratory, 1982b.

(12) L. Vervecken, J. Campsa, J. Meyers., *Accounting for wind-direction fluctuations in Reynolds-averaged simulation of near-range atmospheric dispersion*. Atmospheric Environment, 2013. **72**: p.142-150.